https://doi.org/10.57634/RCR5061

Microwave heating technology for electrolytes of solid oxide fuel cells

Shoufu Yu, Yueyuan Gu, Lei Bi*

School of Resource Environment and Safety Engineering, University of South China, Hengyang 421001, China

The performance of the electrolyte material, being the core component, directly affects the output performance and working temperature of solid oxide fuel cells (SOFCs). However, when conventional high-temperature heating methods are used to prepare electrolytes, many problems arise such as uneven grain growth and element evaporation. To solve these problems, microwave heating (MH) is widely used in the preparation of SOFC electrolytes because of its fast and uniform heating. In this review, the application of MH technology in the preparation and sintering densification of precursors of oxygen ion-conducting SOFC (O-SOFC) electrolytes and proton-conducting SOFC (P-SOFC) electrolytes is reviewed. Furthermore, the superiority of MH technology over conventional heating (CH) technology is emphasized. Examples of high-performance electrolyte materials prepared by microwave sintering are presented. In addition, we also identify various issues that arise with the use of MH technology in the preparation of electrolytes and discuss the future research directions for the application of MH technology in the preparation of electrolytes. The purpose of this review is to draw the community's attention to the application of MH technology to solid oxide fuel electrolytes and to provide valuable guidance for the future development of SOFCs.
The bibliography includes 175 references.

Contents

1. Introduction 1
2. Oxygen-ion conductors 2
2.1. Zirconia-based electrolytes 3
2.2. Yttria-stabilized zirconia 3
2.3. Scandia-stabilized zirconia 3
2.4. Ceria-based electrolytes 5
2.5. Single doping 5
2.6. Double doping and multidoping 6
2.7 $LaGaO_3$-based electrolytes 8
2.8. Other O-SOFC electrolytes 8
3. Proton conductors 9
4. Conclusion 12
5. List of acronyms and designations 12
6. References 13

1. Introduction

Due to the increasingly severe energy crisis, people are urgently seeking efficient and sustainable energy and energy conversion technologies.[1–11] In recent decades, different sustainable and renewable technologies have been proposed, and energy conversion and storage technologies and devices have received intense attention. As devices that can directly convert chemical energy into electrical energy, fuel cells are widely favoured due to their advantages of high energy conversion efficiency, low pollution, and modularity.[12] SOFCs, which are an important type of fuel cells, have become a research hotspot in this field due to their advantages of strong fuel applicability, no electrolyte loss, and absence of use of precious metal catalysts.[13,14] The key materials of SOFCs include electrolyte materials, cathode materials, and anode materials, with electrolyte materials being the core components of SOFCs.[15] The performance of the electrolyte material in a cell directly affects the output performance and working temperature of the cell. In practice, in addition to the mobility of ions in a material, the microstructure of the electrolyte also has a very significant impact on the performance. Most electrolytes are polycrystalline,[16–22] which means that ions need to pass through grains and grain boundaries in the process of conduction,[23–27] as shown in Fig. 1 *a*,*b* depicts a space-charge scheme for polycrystalline materials consisting of a grain-boundary core and two adjacent space-charge layers.[25,26] A large number of oxygen vacancies are present in the grain boundary core, so the potential of the grain boundary nuclei is positive. Under the action of static electricity,[27] the number of oxygen vacancies in the space-charge layer decreases sharply, thus endowing the region with electrical resistance and hindering the transport of ions. Moreover, too many grain boundaries or low electrical conductivity of the grain boundaries reduce the electrical conductivity of a material. The grain and grain boundary properties of electrolytes are closely related to their preparation and sintering methods. Therefore, improving the electrolyte material preparation and sintering methods to reduce or improve the conductivity of grain boundaries is one of the key issues in the development of SOFC electrolytes.

S.Yu. Post-graduate at USC.
Current research interests: proton conductor solid oxide fuel cells.
Y.Gu. Ph.D. in chemistry, Associate Professor at the same University.
Current research interests: electrocatalysis and proton conductor solid oxide fuel cell.
L.Bi. Ph.D. in materials science, Full Professor, Deputy Dean of the School of Resource Environment and Safety Engineering, Professor at the same University.
E-mail: bilei@vip.qq.com; lei.bi@usc.edu.cn.
Current research interests: environmental and energy materials, solid oxide fuel cells.

Received 1 August 2022

© 2022 Uspekhi Khimii, ZIOC RAS, Russian Academy of Sciences

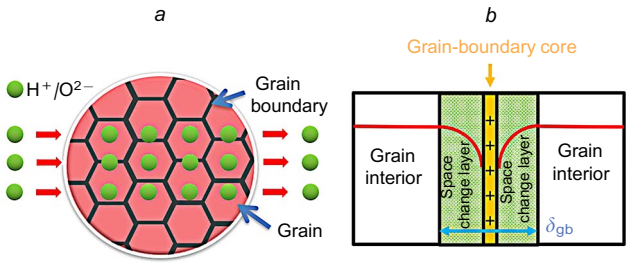


Figure 1. Schematic diagram of ions passing through grains and grain boundaries (*a*) and the space-charge scheme for a polycrystalline material (*b*). Fig.1 *b* was created by the authors based on data of Ref. 25.

Traditional SOFC electrolytes are prepared and sintered in a conventional muffle furnace.[28–30] In the CH method, heat is generated by an external heat source and conducted to the sample to be calcined, so that the sample can reach the required temperature. However, this method, in which heat is transferred from outside to inside, is likely to cause uneven heating of the sample, affecting the densification process and performance of the electrolyte material. Figure 2 *a* is a simple schematic diagram of a traditional heating method. In the past few years, as a new heating method, MH technology has attracted wide attention because of fast-heating speed, which reduces the sintering densification temperatures of electrolyte materials and improves the microstructures of the materials.[31] As shown in Fig. 2 *b*, under the action of the electromagnetic waves of a microwave muffle oven, the electrolyte material produces dielectric loss, resulting in volumetric heating. Compared with traditional sintering, this bulk microwave heating can achieve rapid and uniform heating to form a uniform fine-grained structure inside the material and reach higher densities even at lower sintering temperatures, thereby improving the electrolyte material performance.[32, 33]

Many experimental studies have shown that MH technology can not only effectively reduce the sintering and densification temperatures of an electrolyte to form a uniform grain structure but also effectively inhibit the volatilization of elements, reduce the activation energy and crystallization temperature of the electrolyte, and improve the conductivity of the electrolyte.[34–38] Therefore, this paper summarizes the research progress on the application of MH technology to O-SOFC and P-SOFC electrolytes, highlights its advantages, and identifies its challenges. In addition, this review considers the recent advances in this frontier and dynamic field and provides useful guidance for the future development of SOFCs.

Microwave heating technology is also widely used in the processing and preparation of ceramic materials due to its fast, uniform, and environmentally friendly heating method.[39] In recent years, some researchers have summarized the application of MH in thick ceramics, bioceramics, transparent ceramics, nano-framework ceramics, high-temperature ceramic eutectic materials, and metal-ceramic composites.[39–42] It is concluded that, compared to the CH technology, MH can achieve rapid and high densification of ceramics, limit the coarsening of grains, produce uniform fine-grained structure, and improve the mechanical properties of ceramic materials. These brief reviews did not cover the application of MH in SOFC electrolytes, so the present paper can effectively fill this gap and provide useful guidance for the preparation of SOFC electrolytes by MH.

2. Oxygen-ion conductors

Ideal oxygen ion conductor-based electrolyte materials need to have good oxygen ion conductivity and a very low electronic conductivity. The chemical stability, structural stability, and thermal stability can be maintained in both oxidizing and reducing atmospheres. Maintaining good thermal matching with electrode materials and other contact elements prevents delamination and cracking between layers during cell operation and enables the easy preparation of dense layers to prevent the mutual leakage of fuel gases and oxidizing gases.[43]

Figure 3 illustrates the working principle of a single SOFC with oxygen ion-conducting electrolyte. The chart shows that oxygen, as an oxidizing gas, enters the cathode channel, while hydrogen, as a fuel gas, enters the anode channel. After being adsorbed and dissociated in the negative extreme, oxegen is reduced with electrons to oxygen ion. Then, the oxygen ion enters the electrolyte layer driven by the electrochemical potential difference between the two sides of the electrolyte and transmits to the positive extreme, reacting with fuel to generate water. The released electron is connected to the external circuit through the electrode gain and loss to provide external power. The electrochemical reaction equations are the following:

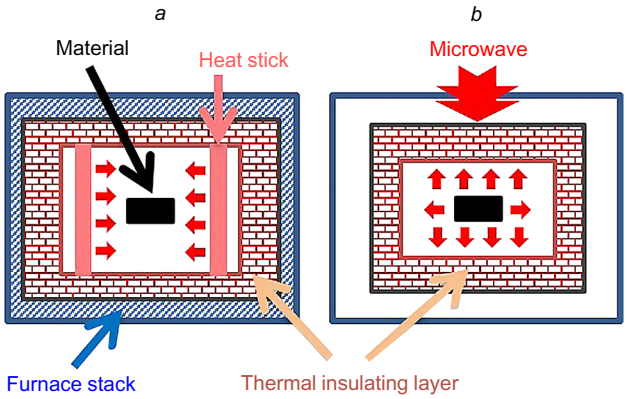


Figure 2. Conventional muffle furnace heating diagram (*a*) and MH diagram (*b*).

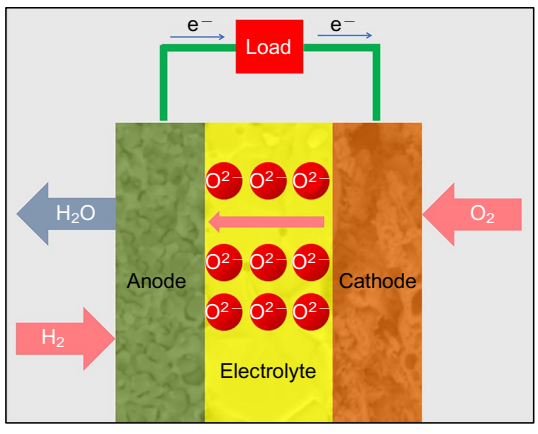


Figure 3. Simplified diagram of the O-SOFC working principle.

Cathode: $O_2 + 4e^- \longrightarrow 2O^{2-}$

Anode: $H_2 + O^{2-} \longrightarrow 2H_2O + 2e^-$

Total reaction: $2H_2 + O_2 \longrightarrow 2H_2O$

2.1. Zirconia-based electrolytes

The zirconia-based electrolyte is the earliest studied O-SOFC electrolyte material and is also one of the most mainstream and thoroughly studied electrolyte materials in SOFCs at high temperatures.[44] Pure ZrO_2 forms a monoclinic crystal system at room temperature; its steric hindrance is fairly significant, and its ion mobility is relatively low, so it has a noticeable specific ion conductivity only at high temperatures. Studies have shown that doping with low-valent elements can make ZrO_2 form a stable cubic structure within the melting point range; at the same time, doping will also generate a large number of oxygen vacancies in the lattice, making ZrO_2 a good oxygen ion conductor. The main doped zirconia-based materials are yttria-stabilized zirconia (YSZ) and scandia-stabilized zirconia (ScSZ).[45–48]

2.2. Yttria-stabilized zirconia

Yttrium oxide is a typical dopant for ZrO_2-based SOFCs. Yttria-stabilized zirconia has become the most classical SOFC electrolyte material because of its good chemical stability, high mechanical strength, and excellent electrical conductivity at high temperatures.[49,50] In addition to the traditional solid-state method, the preparation methods of YSZ include, *inter alia*, the hydrothermal method,[51,52] homogeneous precipitation method,[53,54] and the sol–gel process.[55,56] However, these YSZ preparation methods are often time- and energy-consuming, which limits their commercial viability. In recent years, MH technology has been gradually used in preparing YSZ because of its fast-heating speed, uniform heating, and low sintering densification temperature. Yoshinaga *et al.*[38] successfully synthesized the YSZ precursor by a microwave-assisted homogeneous precipitation method. The precursor prepared by microwave-assisted heating was found to have a smaller particle size and more uniform particle distribution than the precursor prepared by the conventional homogeneous precipitation method. More importantly, the precursor prepared by the above-mentioned procedure was shown to reduce the material crystallization temperature. Many studies have proven that $Zr_{0.84}Y_{0.16}O_{1.92}$ (8YSZ) has better performance.[57] To further improve the electrical conductivity of YSZ, Vijay *et al.*[58] prepared an 8 mol.% YSZ precursor by a microwave-assisted gel combustion method. Studies have shown that 8 mol.% YSZ precursors thus prepared have higher electrical conductivities than those obtained by conventional methods. This is mainly due to the fact that 8 mol.% YSZ precursors prepared by microwave-assisted gel combustion have a smaller particle size than those prepared by traditional methods. The smaller grain size corresponds to a higher surface energy, resulting in a good growth process under high-temperature sintering, which can effectively improve the electrochemical performance of the electrolyte.

The MH technology is widely used not only to obtain YSZ precursors, but also for the sintering and densification of electrolytes. Singh *et al.*[59] prepared YSZ ($Zr_{1-x}Y_xO_{2-x/2}$) precursors of different compositions by co-precipitation method. Sintering was performed in a microwave muffle furnace at 1400 °C for 20 min and in a conventional muffle furnace at 1400 °C for 240 min. The research results showed that both sintering methods yielded electrolyte materials with good densities and comparable electrical conductivities. However, the dwelling time was significantly reduced by using the microwave sintering method, demonstrating that the use of this technology can save significant time and energy without affecting the quality of the material.

Good mechanical properties guarantee electrolyte safety and are conducive to the trend towards electrolyte thinning and industrial production. Chen *et al.*[60] studied the mechanical properties of electrolytes prepared by $La_2O_3-Y_2O_3-ZrO_2$ co-doping under microwave sintering conditions. As can be seen from Fig. 4, the doping of La_2O_3 reduced the grain size of the material, and the higher the amount of the dopant, the smaller thegrain size. Generally, the smaller the grain size, the lower the fracture toughness. However, the microwave sintered sample (average particle size of 500 nm) had a higher fracture toughness than the conventional sample (average particle size of 700 nm). The main reason for this phenomenon may be that microwave sintering reduces the grain boundary strength of the $La_2O_3-Y_2O_3-ZrO_2$ ceramics and induces the formation of intergrain fractures in the microwave-sintered $La_2O_3-Y_2O_3-ZrO_2$ samples, which increases the crack propagation path length and improves the fracture toughness of the materials.

2.3. Scandia-stabilized zirconia

Since YSZ meets almost all requirements to SOFC materials, it is the best choice for SOFC electrolyte materials under high-temperature conditions. However, as an electrolyte material, YSZ has a low conductivity at intermediate temperatures (below 10^{-3} S cm^{-1} at 600 °C), which hinders the application of YSZ electrolyte materials to intermediate-temperature SOFCs.[61] Zirconia was doped with Sc to obtain a new electrolyte, scandia-stabilized zirconia. Its electrical conductivity reached 0.1 S cm^{-1} at 750 °C, and the material showed good stability in both oxidizing and reducing atmospheres, which meets the requirements for

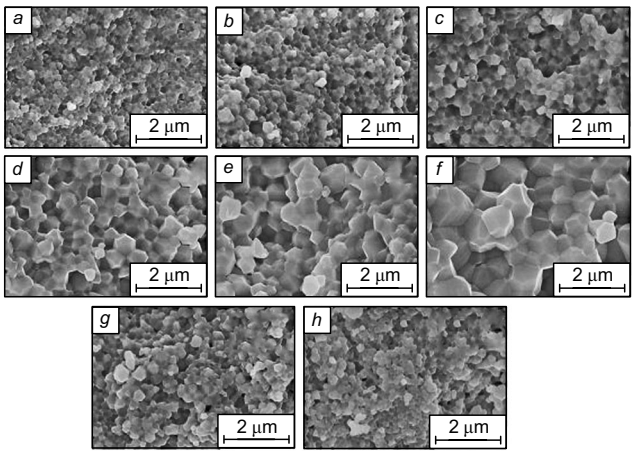


Figure 4. Fracture surfaces of 3Y–nLa-PSZ compacts sintered by microwave heating at different temperatures: 3Y–1La-PSZ, 1400 °C (*a*); 3Y–1La-PSZ, 1450 °C (*b*); 3Y–1La-PSZ, 1500 °C (*c*); 3Y–1La-PSZ, 1550 °C (*d*); and 3Y–1La-PSZ, 1600 °C (*e*); 3Y–0La-PSZ, 1550 °C (*f*); 3Y–3La-PSZ, 1550 °C (*g*); and 3Y–5La-PSZ, 1550 °C (*h*).[60] Reproduced with permission from Elsevier.

intermediate-temperature SOFC electrolyte materials.[62, 63] Ao *et al.*[64] prepared a ScSZ powder by the microwave-hydrothermal method. It was found that the crystallization temperature of the synthesized material was effectively reduced under MH conditions and that the crystallinity of the ScSZ material was positively related to the MH time. The use of MH at 150 °C for 2.5 h provided a nanometre-sized cubic ScSZ powder with good crystallinity (Fig. 5 *a*). Compared with the conventional hydrothermal method, which usually takes 1 to 7 days, the reaction time was greatly shortened, as illustrated in Fig. 5 *b*. Sharma *et al.*[65] prepared $Zr_{0.9}Sc_{0.1}O_{1.95}$ (10ScSZ) by the solid-state method. The densification time and electrochemical performance of 10ScSZ (10SSZ-MW) prepared by microwave sintering at the same sintering temperature were compared with those of 10ScSZ (10SSZ-CON) prepared by conventional sintering (CON). The results showed that the 10SSZ-MW obtained by microwave sintering in 20 min had the same completely stable cubic phase as 10SSZ-CON obtained by conventional sintering in 6 h. As can be seen from Table 1, 10SSZ-MW had higher density and electrical conductivity than 10SSZ-CON. The potential of microwave sintering in the processing of electrolyte materials and the cost-effectiveness in terms of time and energy savings were demonstrated.

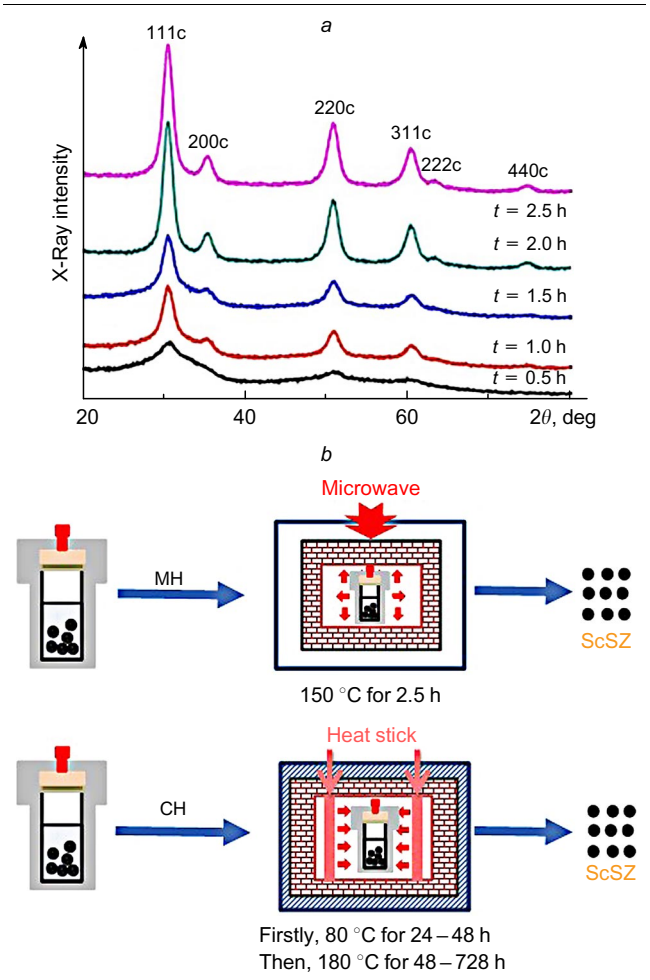


Figure 5. X-ray diffraction patterns of ScSZ powders prepared at 150 °C (c is cubic phase) (*a*);[64] comparison scheme of microwave–hydrothermal and hydrothermal preparation of ScSZ (*b*). Reproduced with permission from Elsevier.

Table 1. Values of ionic conductivity at 500 °C and density.[64]

Sample	Density, g cm^{-3}	Conductivity, S cm^{-1}
10SSZ-MW	5.46	1.46×10^{-3}
10SSZ-CON	5.12	8.18×10^{-5}

Stable cubic-phase ScSZ is considered to be an excellent intermediate-temperature SOFC (IT-SOFC) electrolyte material. However, in the practical application, it was found that ScSZ was prone to phase transition at the working temperature ranging from 500 °C to 700 °C, from the cubic phase to the rhombohedral or tetragonal phase, and its electrical conductivity decreased by at least one order of magnitude.[66, 67] Therefore, improving the stability of ScSZ at low temperatures is a hot topic of current research. Co-doping is a method that is often used to enhance the stability of zirconia.[48, 68] CeO_2 doping of fluorite structures is a relatively mature method. The introduction of Ce^{4+}, which has a larger ionic radius (0.97 Å), can improve the stability of cubic zirconia and inhibit its transition to the rhombohedral or tetragonal phase.[69, 70] Studies have shown that 10 mol.% Sc_2O_3 – 1 mol.% CeO_2 – 89 mol.% ZrO_2 (10Sc1CeSZ) can maintain the cubic phase with high conductivity at the IT-SOFC working temperature.[71] At the same time, the performance of the 10Sc1CeSZ electrolyte is greatly affected by the powder characteristics of the precursor. Therefore, the performance of the 10Sc1CeSZ electrolyte can be improved by optimizing the powder characteristics. Moreover, powder properties such as the particle size, surface area, and purity are mainly affected by the synthesis and preparation methods, and electrolyte materials with superiour properties can be obtained by suitable preparation methods.[72] Jais *et al.*[73] prepared ultrafine 10Sc1CeSZ powders with a particle size of 20 nm and a specific surface area of 16 m^2 g^{-1} by the microwave-assisted glycine–nitrate method (MW-GNM). This method produces less organic matter in the process of microwave-assisted heating and combustion. Hence, this method provides 10Sc1CeSZ with a lower weight loss rate and higher yield compared to the traditional sol–gel method, precipitation method, and the improved Pechini method. The powder had a high density and electrical conductivity after conventional sintering at 1400 °C for 5 h. When the measuring temperature was 800 °C, the ionic conductivity of the 10Sc1CeSZ electrolyte reached 0.184 S cm^{-1}, which was much higher than those of similar electrolytes. The results showed that the properties of 10Sc1CeSZ electrolytes can be improved by the MH technology.

Although the 10Sc1CeSZ electrolyte satisfies most of the conditions for its application in IT-SOFC, its higher sintering densification temperature and longer sintering time limit the development of its commercial applications. Therefore, efforts should be made to develop a low-temperature and rapid-sintering preparation method to improve its practical application value. Ng *et al.*[74] sintered a 10Sc1CeSZ electrolyte in a microwave muffle furnace (1300 and 1350 °C, 15 min) and in a conventional muffle furnace (1300–1550 °C, 2 h). The effects of the conditions of these two methods on the properties of the resulting 10Sc1CeSZ electrolyte were studied. The results showed that both sintering methods yielded stable cubic-phase ZrO_2. Figure 6 presents SEM images of the products of these two methods at different temperatures. According to the

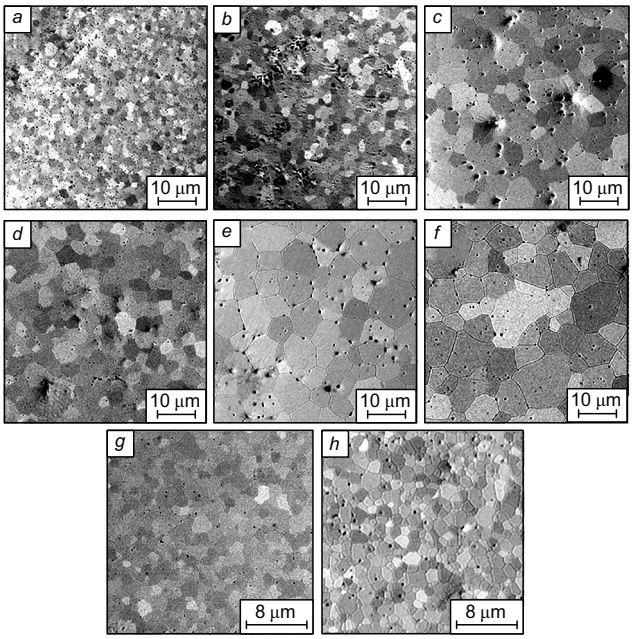


Figure 6. SEM images of 10Sc1CeSZ samples conventionally sintered at 1300 °C (*a*), 1350 °C (*b*), 1400 °C (*c*), 1450 °C (*d*), 1500 °C (*e*), and 1550 °C (*f*) and microwave-sintered at 1300 °C (*g*) and 1350 °C (*h*).[74] Reproduced with permission from Elsevier.

Figure, both sintering methods produced dense electrolyte materials, with their densities exceeding 98%. However, the decrease in grain size was assumed to increase the interface between the grains and the grain boundary resistance; hence, the electrical conductivity of the microwave-sintered 10Sc1CeSZ was expected to be slightly lower than that of conventionally sintered 10Sc1CeSZ. However, in this study, the authors found that microwave sintering significantly improved the grain boundary diffusion and transport ability of charged particles at high temperatures and reduced the barrier to charged particle migration. Therefore, the electrical conductivity (0.314 S cm^{-1}) of 10Sc1CeSZ prepared by microwave sintering at 800 °C was higher than that of conventionally sintered 10Sc1CeSZ (0.280 S cm^{-1}).

To show more clearly the effect of MH on the properties of zirconia-based electrolytes, Fig. 7 summarizes the conductivity values of electrolytes prepared by the MH and CH methods. It is obvious that the electrolyte prepared by MH has higher conductivity than that prepared by CH heating. In addition, it has been proven that the MH technology can effectively improve the performance of electrolytes.

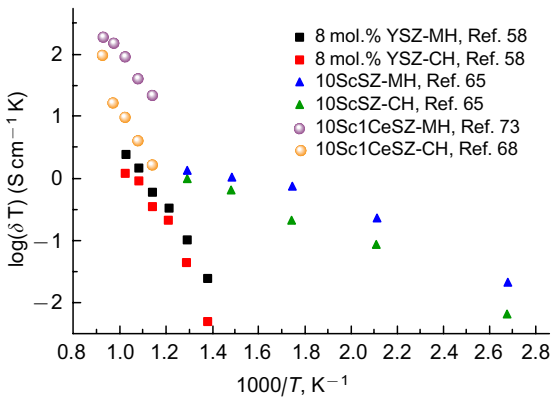


Figure 7. The conductivity of zirconia-based electrolytes prepared by the MH and CH techniques. The Figure was created by the authors based on data of Refs 58, 65, 68, and 73.

2.4. Ceria-based electrolytes

Ceria-based electrolytes are currently the most commonly used materials for intermediate-temperature SOFCs due to the high oxygen-ion conductivity of doped CeO_2 at intermediate temperatures.[75,76] Pure CeO_2 is a cubic fluorite phase that, like ZrO_2, has lower ionic conductivity and higher sintering densification temperature. Researchers hoped to solve these problems by optimizing the synthesis of CeO_2. For example, Carregosa *et al.*[77] prepared nano-CeO_2 by microwave-hydrothermal technology. The sintering densification temperature was reduced from 1500 °C to 1200 °C, and the electrical conductivity increased from 0.33×10^{-5} S cm^{-1} to 2.14×10^{-5} S cm^{-1}. However, the latter parameter was still low, which limited the application of the above-mentioned material in solid fuel cell electrolytes. It was found that the ionic conductivity of CeO_2 could be improved by introducing low-valent rare earth ions or alkaline earth metals. Currently, the state-of-the-art doping methods mainly include single doping, co-doping, and multidoping.[78,79] In addition to doping with suitable low-valent ions, the preparation method, sintering temperature, and sintering time also greatly influence the properties of electrolyte materials.[80,81] Optimizing the preparation method of CeO_2-based materials and the sintering method can also improve the electrolyte performance. The traditional approaches to CeO_2-based materials mainly comprise the solid-state method,[82] co-precipitation method,[83] hydrothermal method,[84] and combustion method.[85] Although these methods enable the preparation of pure-phase CeO_2-based materials, their implementation is often time-consuming. It is difficult to control the uniformity of the prepared materials, and they easily agglomerate. In recent years, microwave-assisted synthesis technology for preparing CeO_2-based materials has become a highly controllable method for preparing CeO_2-based nanopowders. Compared with CH technology, this method can produce smaller particles with a narrower particle size distribution in a short time.[86,87] The more uniform CeO_2-based material prepared by this method not only leads to an increase in the sintering activity[88] of the material but also reduces the sintering temperature. In addition, the activation energy is decreases with enhanced electrical conductivity.[89–92]

2.5. Single doping

In recent years, a lot of attention has been focused on the study of single-doped CeO_2-based electrolytes. Charge compensation is realized by doping bivalent or trivalent ions into ceria electrolytes to form high-concentration oxygen vacancies. Under the same doping conditions, CeO_2-based electrolytes show higher conductivity than ZrO_2-based electrolytes.[76,93] Since Gd^{3+}, Sm^{3+}, Nd^{3+}, Dy^{3+}, *etc.* and Ce^{4+} have similar ionic radii, gadolinium-doped ceria (GDC), samarium-doped ceria (SDC), neodymium-doped ceria (NDC), and dysprosium-doped ceria (DDC) are also the most widely studied single-doped CeO_2-based electrolyte materials.[94–97] Shaikh and Rode[98] prepared $Gd_{0.1}Ce_{0.9}O_{1.95}$ (10GDC) materials by microwave-assisted glycine-nitrate method. The effects of different sintering temperatures on the crystallite size, morphology, and elec-

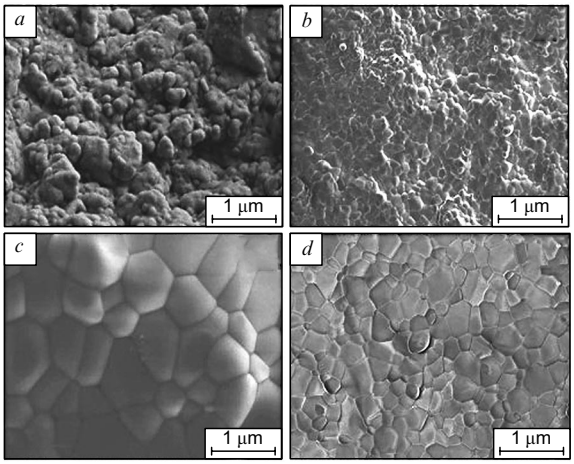


Figure 8. Field-emission scanning electron microscopy (FESEM) images of 10GDC sintered at 800 °C (*a*), 900 °C (*b*), 1000 °C (*c*), and 1200 °C (*d*) for 4 h.[98] Reproduced with permission from the Royal Society of Chemistry.

trical conductivity of 10GDC electrolytes were studied. The results showed that the 10GDC materials prepared by MW-GNM were of nanoscale crystallite size. Microcrystalline particles grew at 800 °C, and good densification performance was reached after treatment for 4 h at 1000 °C, which is much lower than the densification temperatures used in traditional sintering methods. As shown in Fig. 8, the nucleation of 10GDC particles was fast and uniform under the MH conditions. The uniform grains formed an ordered structure of oxygen vacancies, which expanded the conduction path of oxygen ions through the grain boundary and improved the grain boundary conductivity of the material. The maximum ionic conductivity of the material was 3.55×10^{-1} S cm^{-1} for test temperature of 800 °C and O_2 ambient atmosphere.

To further explore the primary role of MH technology in the single-doped CeO_2-based electrolytes, Acharya[99] prepared and sintered $Ce_{1-x}Dy_xO_{2-x/2}$ (DDC100X) by MH and CH techniques. It was found that compared with CH technology, MH enablesrapid and efficient preparation and sintering of DDC100X materials while saving a significant amount of energy. Most importantly, the nano-DDC100X grains prepared by MH technology were smaller and more uniformly distributed. The smaller grains had higher surface energies, enabling a good growth process during high-temperature sintering, which effectively improved the electrochemical performance of the electrolyte. DDC15 prepared by microwave sintering at 1050 °C for 1h has an ionic conductivity of 7.42×10^{-2} S cm^{-1} and an activation energy of 0.86 eV at 500 °C. In contrast, DDC15 prepared by conventional sintering at 1300 °C for 5 h has a conductivity of 9.79×10^{-3} S cm^{-1} and an activation energy of 1.05 eV at 550 °C. At the same time, the researchers compared the variations in the sintering properties of DDC15 materials with temperature for the MH and CH technologies. The results showed that the sintering properties of DDC15 materials had a linear relationship with temperature under the MH conditions. In contrast, a nonlinear relationship was observed in the case of CH, further proving that MH provides uniform heating of materials. This was also the main reason why the grains of the materials obtained by microwave sintering were more uniform than those obtained by conventional sintering.

The fast-sintering feature of MH could be useful for preventing the volatilization of elements. Bismuth-doped CeO_2-based electrolyte materials have high ionic conductivity and good application prospects in the development of low-temperature SOFCs.[100] However, due to the low volatilization temperature of Bi, during sintering at temperatures above 835 °C for a long time, Bi is easily volatilized, which severely reduces the performance of the electrolyte. To address this issue, Prekajski *et al.*[101] managed to prepare dense $Ce_{1-x}Bi_xO_{2-\delta}$ electrolyte materials by microwave sintering at 1050 °C for 1 h. Due to the fast and uniform heating mode of the microwave oven, $Ce_{1-x}Bi_xO_{2-\delta}$ effectively avoided the volatilization of Bi at a sintering temperature of 1050 °C for 1 h. It was also found that $Ce_{1-x}Bi_xO_{2-\delta}$ electrolyte materials prepared by microwave sintering at 1050 °C had a higher density, finer grain size, and more uniform grain distribution than those sintered at 1450 °C in a muffle furnace. Moreover, the effect of doping amount of Bi on the electrical conductivity was studied for microwave sintering at 1050 °C. The results are shown in Table 2. According to the data, when the doping concentration of Bi element was 20%, the resulting material had a higher electrical conductivity. For a test temperature of 700 °C, the total conductivity was $\sim 3.27 \times 10^{-3}$ S cm^{-1}.

2.6. Double doping and multidoping

Although the single-doped CeO_2-based material has been shown to have high ionic conductivity, it may generate electronic conductivity at low oxygen partial pressures and high temperatures, which limits its practical applications. Co/multidoping cations can not only reduce the electronic conductance and hinder the ordering of oxygen vacancies, but also regulate the lattice distortion of a ceria solid solution.[102, 103] At the same time, due to the charge compensation effect, the number of oxygen vacancies in the material increases thus further enhancing the ionic conductivity of the material. The co-doped $Ce_{0.8}Sm_{0.2-x}Y_xO_{2-\delta}$ electrolyte prepared by conventional sintering was found to haveahigher electrical conductivity and a lower activation energy than single-doped $Ce_{0.8}Sm_{0.2}O_{2-\delta}$.[104] The similar phenomenon was also observed in the Dy^{3+}/Sc^{3+} co-doped system, confirming the advantage of the co-doping method.[105] To further improve the performance of the $Ce_{0.8}Sm_{0.2-x}Y_xO_{2-\delta}$ electrolyte material, Venkataramana *et al.*[106] prepared a $Ce_{0.8}Sm_{0.2-x}Y_xO_{2-\delta}$ (CSY100X) electrolyte material using sintering at 1200 °C for 1 h in a microwave muffle furnace. Comparison of this material with $Ce_{0.8}Sm_{0.2-x}Y_xO_{2-\delta}$ prepared in a conventional muffle furnace by sintering at 1300 °C (CSY100XC) by

Table 2. Bulk (k_b) and grain boundary (k_{gb}) ionic conductivities of the sample $Ce_{0.8}Bi_{0.2}O_{2-\delta}$ and total ionic conductivity (k_{b+gb}) of the sample $Ce_{0.5}Bi_{0.5}O_{2-\delta}$ obtained by microwave sintering at 1050 °C.[101]

T, °C	$Ce_{0.8}Bi_{0.2}O_{2-\delta}$		$Ce_{0.5}Bi_{0.5}O_{2-\delta}$
	k_b, S cm^{-1}	k_{gb}, S cm^{-1}	k_{b+gb}, S cm^{-1}
600	1.62×10^{-3}	3.52×10^{-4}	1.89×10^{-4}
625	2.03×10^{-3}	4.98×10^{-4}	2.45×10^{-4}
650	2.74×10^{-3}	6.67×10^{-4}	4.74×10^{-4}
675	2.83×10^{-3}	7.62×10^{-4}	7.85×10^{-4}
700	3.14×10^{-3}	9.32×10^{-4}	1.23×10^{-3}

Table 3. Electrical conductivity, grain activation energy (E_{ag}), and grain boundary activation energy (E_{agb}) of CSY100X and CSY100XC at 500 °C.[106]

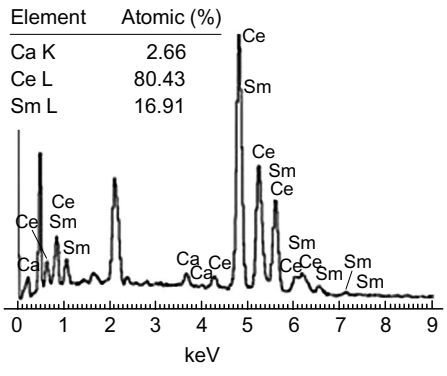
Sample	Conductivity, S cm^{-1}	E_{ag}, eV	E_{agb}, eV
CSY100X	0.011	0.49	0.54
CSY100XC	0.0069	0.51	0.56

Raman analysis showed that microwave sintering increased the number of oxygen vacancies in the material. As illustrated in Table 3, CSY100X had a higher conductivity and a lower activation energy than CSY100XC. The main reason for this result may be that a larger number of oxygen vacancies is beneficial for the conduction process of oxygen ions and reduce the activation energy of ions.

Yttrium and dysprosium co-doped CeO_2-based electrolytes can better inhibit the electronic conductivity produced by single-doped CeO_2-based electrolytes at high temperatures. Nevertheless, the Y and Dy co-doped CeO_2-based electrolytes often need higher sintering densification temperatures ($\geqslant$1400 °C) and longer sintering times ($\geqslant$4 h).[107] To reduce the sintering temperature of Y and Dy co-doping, decrease the sintering time and improve its practical application value, Madhusudan *et al.*[108] prepared $Ce_{0.8}Y_{0.2-x}Dy_xO_{2-\delta}$ electrolyte materials by the sol–gel method, and the densification temperatures of the Y and Dy co-doped CeO_2-based electrolytes were greatly reduced by microwave sintering. The relative densities of all $Ce_{0.8}Y_{0.2-x}Dy_xO_{2-\delta}$ electrolytes sintered at 1300 °C for 30 min reached more than 95%. Using Raman spectroscopy it was additionally confirmed that the doping amount could increase the oxygen vacancy concentration, which facilitates the mobilities of the oxygen ions, thus improving the material conductivity.

Relatively few studies have been conducted on multi-doped ceria electrolyte materials. Venkataramana *et al.*[109] experimented with multidoping of ceria, and used Pr^{3+}, Sm^{3+}, and Gd^{3+} to replace some Ce^{4+} ions to give new $Ce_{1-x}(Pr_{1/3}Sm_{1/3}Gd_{1/3})_xO_{2-\delta}$ electrolyte materials. The research results showed that $Ce_{0.76}Pr_{0.08}Sm_{0.08}Gd_{0.08}O_{2-\delta}$ had the highest ionic conductivity (1.86×10^2 S cm^{-1}) and the lowest activation energy (0.56 eV) for working temperature of 600 °C. At the same time, the thermal expansion coefficient of $Ce_{0.76}Pr_{0.08}Sm_{0.08}Gd_{0.08}O_{2-\delta}$ at 30–1000 °C was consistent with those of commonly used electrode materials, and it had excellent practical application value. To further improve the performance of the $Ce_{0.76}Pr_{0.08}Sm_{0.08}Gd_{0.08}O_{2-\delta}$ electrolyte, the sintering densification temperature and the sintering densification time were reduced. In the follow-up study,[110] the effects of the sintering time on the electrochemical properties of materials were further explored by using microwave sintering technology (samples sintered at 1300 °C with sintering times of 15, 30, and 60 min were named PSG-MS15, PSG-MS30, and PSG-MS60, respectively). The results showed that the microwave sintering time dramatically influenced the number of oxygen vacancies and electrical conductivity of the material. Too short or too long sintering times did not contribute to the formation of oxygen vacancies, thereby further affecting the electrical conductivity of the material. The results showed that microwave sintering for 30 min was the most beneficial method in terms of the grain boundary resistance and electrical conductivity of the materials. Compared with the material produced by the traditional sintering method, PSG-MS30 had more oxygen vacancies and a higher electrical conductivity. The electrical conductivity of the material was 3.47×10^{-2} S cm^{-1} at 600 °C, which was nearly twice that of the material produced by the traditional sintering method.

It is believed that microwave sintering can effectively reduce the grain size, decrease the activation energy of the grain boundary, and improve the grain boundary conductivity of the material. However, most of this research is based on the microwave sintering temperature being lower than the conventional sintering temperature. Prado-Gonjal *et al.*[111] prepared Sm and Ca co-doped $Ce_{0.8}Sm_{0.18}Ca_{0.02}O_{1.9}$ electrolyte materials by the microwave-hydrothermal method and studied the effects of the MH and CH methods on the properties of the $Ce_{0.8}Sm_{0.18}Ca_{0.02}O_{1.9}$ electrolyte at the same sintering temperature. In contrast to the previous data,[74,99] the authors found that although microwave sintering could produce dense $Ce_{0.8}Sm_{0.18}Ca_{0.02}O_{1.9}$ electrolyte materials relatively quickly and efficiently (Fig. 9), at the same sintering temperature, with increased sintering time, the resulting grain size was similar to that obtained by conventional sintering, and there were no smaller nanosized grains than in previous studies.[38,99] This conclusion is consistent with findings of Chen *et al.*[60] that microwaves can inhibit grain boundary energy growth in a short time, but after a threshold time,



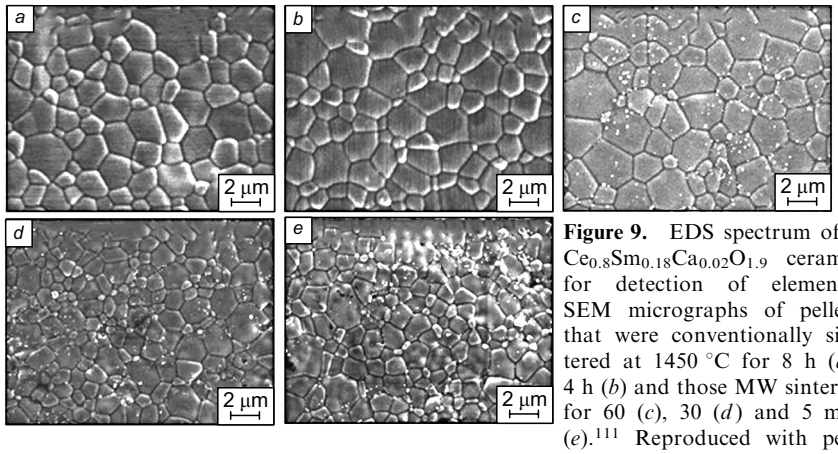


Figure 9. EDS spectrum of a $Ce_{0.8}Sm_{0.18}Ca_{0.02}O_{1.9}$ ceramic for detection of elements. SEM micrographs of pellets that were conventionally sintered at 1450 °C for 8 h (*a*), 4 h (*b*) and those MW sintered for 60 (*c*), 30 (*d*) and 5 min (*e*).[111] Reproduced with permission from Elsevier.

the grains overgrow due to the accumulation of energy at the grain boundaries.

2.7 $LaGaO_3$-based electrolytes

Perovskite-structured oxides (ABO_3) are electrolyte materials with good performance due to their ion electronic mixed conductivities. Perovskite oxides $LaBO_3$ (B = Al, Sc, Ga, Y, *etc.*) exhibit high oxygen ion conductivities at moderate temperatures,[112] among which $LaGaO_3$-based solid oxide is the most studied perovskite oxide electrolyte.[113, 114] Ishihara *et al.*[115] and Huang and Petric[116] reported the preparation of a double-doped $La_{0.9}Sr_{0.1}Ga_{0.8}Mg_{0.2}O_{3-\delta}$ (LSGM) electrolyte material, which is a pure oxygen ionic conductor over a wide range of oxygen partial pressures. Its ionic conductivity at 800 °C was similar to that of 8YSZ at 1000 °C. Therefore, owing to their excellent oxygen ion conductivities at moderate temperatures, LSGM perovskite oxides have attracted the interest of both domestic and foreign researchers,. The preparation method directly affects the purity and grain size of LSGM powders and determines the performance of electrolytes in cells. In addition to the traditional solid-state method,[117, 118] the sol–gel method,[119, 120] Pechini method,[121] glycine nitrate combustion method,[122, 123] solution polymerization,[124, 125] and other preparation techniques have been used to improve the performance of LSGM. Although these new preparation techniques have improved the electrolyte performance, due to the narrow stable composition range of the LSGM phase, if the composition deviates from the ideal composition, secondary phases will be generated (such as $LaSrGa_3O_7$ and $LaSrGaO_4$), which, in turn, will degrade the mechanical and electrochemical properties of LSGM.[126] Moreover, the LSGM powder easily agglomerates, and a higher density can be obtained by sintering at 1400–1500 °C for 15 to 35 h; hence, the grain size of the prepared LSGM electrolyte films exceeded 20 μm. To improve the sintering purity of LSGM, reduce the high-temperature sintering time and decrease the grain size, Zhai *et al.*[127] prepared higher-purity $La_{0.8}Sr_{0.2}Ga_{0.83}Mg_{0.17}O_{2.815}$ ($LS_{0.2}GM_{0.17}$) by a microwave-assisted Pechini method (MWP). The results showed that due to the rapid and uniform bulk microwave heating method, the esterification of citric acid and ethylene glycol took place simultaneously in the solution, thereby reducing the segregation phenomenon that easily occurred in the traditional Pechini method. At the same time, due to the rapid esterification reaction (which took no more than ten minutes), the particle size of the prepared precursor powder was smaller and more uniform, which was beneficial for the densification process of the material. Based on the findings of Zhai *et al.*,[127] Boldrini *et al.*[128] further studied the effect of MWP on the electrochemical performance of $LS_{0.2}GM_{0.17}$. The conductivity of the thus prepared $LS_{0.2}GM_{0.17}$ was about 4.38×10^{-2} S cm^{-1} at 700 °C, which was higher than that of LSGM prepared by the traditional Pechini method ($\sim3.25\times10^{-2}$ S cm^{-1} at 700 °C). This indicates once again that microwave-assisted heating can not only improve the efficiency and reduce the cost but also improve the performance of the electrolyte.

It was found that the above-mentioned microwave-assisted Pechini method[127] consumes a large amount of organic matter, resulting in an unavoidable waste of resources; hence, the researchers used an improved polyvinyl alcohol (PVA) technology to prepare $LS_{0.2}GM_{0.17}$ based on microwave-assisted heating to reduce the waste of organic matter and improve the performance of electrolytes.[129] A key point of this method was the use of an appropriate amount of PVA, which can provide the uniform distribution of metal ions due to its long chain. Too large or too small amount of PVA can hamper the desired distribution, and unnecessary secondary phases will be produced in the sintering process. By studying the effect of the amount of PVA on the purity of the product, the researchers determined that the best dosage of PVA was $Me^{n+}/-OH^- = 1.65:1$, which ensured that the pure phase and dense electrolyte material with a grain size of 2–3 μm could be obtained by sintering at 1400 °C for 9 h.

Although various excellent preparation techniques were used to prepare LSGM, under traditional sintering conditions, LSGM still needs a higher sintering temperature and longer sintering time to achieve a higher density. The grain size increases gradually with the high-temperature sintering time, and secondary phases such as $SrLaGa_3O_7$ and $La_4Ga_2O_9$ are often detected at the grain boundary.[130] Kesapragada *et al.*[131] used microwave sintering instead of conventional sintering technology to effectively address this problem. Thus, LSGM electrolyte materials with a grain size of 2–3 μm and a density of ⩾95% were successfully prepared under microwave sintering conditions at 1350 °C for 20 min. This procedure reduce the sintering temperature, significantly decreases the sintering time, and increases the preparation efficiency of such materials. Moreover, due to the short process time, it is devoid of the formation of secondary phases such as $SrLaGa_3O_7$ and $La4Ga_2O_9$ and improves the electrochemical performance of materials. Moure *et al.*[132] also proved experimentally that the existence of $SrLaGa_3O_7$ and $La_4Ga_2O_9$ can reduce the electrical conductivity. The results showed that the conductivity of the pure phase LSGM material was $\sim1.27\times10^{-3}$ and the conductivity of impurity-containing $SrLaGa_3O_7$ was $\sim5.24\times10^{-4}$ under the test condition of 450 °C.

2.8. Other O-SOFC electrolytes

Electrolytes ($La_{10}(MO_4)_6O_2$, M = Ge, Co, Si, Al, or P) with an apatite-type structure have received increasing attention as new electrolyte materials due to their high ionic conductivity and good matching of electrode materials.[133, 134] However, the sintering activity of apatite-type electrolytes is poor, and the sintering densification temperature for the traditional sintering method is ⩾1600 °C. In particular, the prolonged exposure of $La_{9.33}Si_2Ge_4O_{26}$ oxide apatite, having an increased La/Ge atomic ratio, to elevated sintering temperatures easily causes Ge volatilization and formation of the insulating La–Ge oxides (such as La_2GeO_5).[135] Therefore, to prevent Ge from volatilizing at a temperature > 1250 °C, the sintering process should proceed rapidly and at a relatively low temperature. To solve this problem, Santos *et al.*[136] prepared dense $La_{9.33}Si_2Ge_4O_{26}$ electrolyte materials by microwave heating at 1300 °C and 1350 °C for 1 h, respectively. According to the experimental results, the electrolyte materials prepared at these sintering temperatures can effectively inhibit the volatilization of Ge and have the same apatite structure with relative densities of 92% and 96%, respectively. The mechanical analysis of the sintered materials shows that the hardness, Young's modulus, yield strength, and fracture toughness of the sintered materials are 7.1 and 8.0 GPa, 122 and 133 GPa and 1807 and 2073 MPa, respectively.

$La_2Mo_2O_9$ has attracted considerable attention because of its high ionic conductivity under medium and low-temperature conditions and a wide range of oxygen partial pressure.[137–139] Saradha *et al.*[140] successfully prepared single-phase $La_2Mo_2O_9$ electrolyte materials by microwave-assisted combustion synthesis. The resulting material was characterized by good sintering activity; a dense electrolyte material can be obtained after sintering at 800 °C for 5 h, with itsrelative density being up to 97%. The conductivity of the compact $La_2Mo_2O_9$ was 0.15 S cm^{-1} at 750 °C, and the ion transfer number was more than 0.99 in the temperature range of 600 to 800 °C. This compound undergoes a phase transition from a slightly monoclinic low-temperature α-phase to a cubic high-temperature β-phase at about 580 °C. To address this issue and further improve the electrical conductivity of the material, in the follow-up study, microwave-assisted combustion synthesis was employed to prepare $La_{2-x}Sm_xMo_2O_9$ electrolyte materials.[141] It was found that the resulting electrolyte material $La_{1.7}Sm_{0.3}Mo_2O_9$ could be sintered at 800 °C for 5 h, and its relative density was up to 98%. The doping with Sm can not only enhance the electrical conductivity of the material (0.196 S cm^{-1} at 750 °C), but also effectively inhibit the phase transition in the material and improve the material practical application value.

3. Proton conductors

Traditional high-temperature O-SOFCs have been developed for many years, their preparation technology is well-developed, and their performance is superiour at high temperatures. However, the high operating temperature can cause various safety issues, as well as problems with gas handling and routine maintenance, preventing its practical application from being popularized.[142, 143] The development of intermediate-temperature and low-temperature fuel cells is an inevitable trend because the working conditions of medium and low temperatures can improve the stability of cell materials, which is beneficial for the commercial applications of SOFCs.[144–151] Therefore, the development of novel medium and low-temperature P-SOFC electrolytes and electrodes has gradually become a research hotspot.[152–156] Such materials have many unique advantages: (1) since the proton radius is smaller than that of oxygen ions, and it is easier to conduct in oxides, so proton conductor oxides have lower activation energies than traditional oxygen ion conductors; (2) P-SOFC electrolyte materials have higher conductivity at lower temperatures; when used in a cell, P-SOFCs can effectively avoid the increase in ohmic resistance caused by decreasing temperature and conductivity. (3) H_2O in P-SOFC is generated on the cathode side, which effectively prevents the dilution of the anode fuel gas by H_2O and improves the fuel utilization rate, as illustrated in Fig. 10.

However, MH technology had rarely been used in P-SOFC until now. Considering that sintering and elemental evaporation are two problems arising in the case of the traditional proton-conducting oxides, MH may have substantial potential. $BaCe_{0.7}Zr_{0.1}Y_{0.2}O_{3-\delta}$ (BCZY) material is one of the most widely used electrolytes in proton conductor solid oxide fuel cells because of its high electrical conductivity and good chemical stability. Barison *et al.*[157] prepared $BaCe_{0.65}Zr_{0.20}Y_{0.15}O_{3-\delta}$ (BCZY15) powders with the microwave-assisted sol–gel Pechini method (MW-SGP). The results showed that, compared with traditional SGP preparation technology, due to the fast and uniform heating mechanism, the preparation time was significantly reduced from two days to 3.5 h, which dramatically improved the energy efficiency. At the same time, under the same sintering conditions, the BCZY15 prepared by MW-SGP has higher density and larger grain size than the BCZY15 prepared by simple SGP, which were more in line with the requirements for a suitable electrolyte.

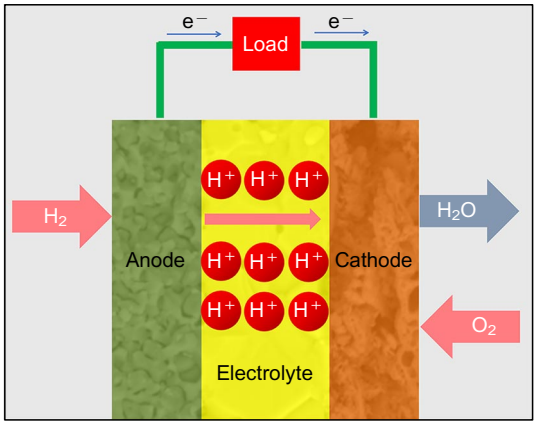


Figure 10. Simplified diagram of the P-SOFC working principle.

The sintering activity of $BaCeO_3-BaZrO_3$-based proton conductors is generally poor. Although sintering aids can greatly improve the sintering activity of these materials, they will adversely affect the electrochemical properties of the materials, *e.g.*, by introducing electronic conductivity and reducing the ionic conductivity.[158] Electrolytes based on $BaCeO_3-BaZrO_3$ without sintering aids need higher sintering temperatures, which will lead to the volatilization of Ba elements and reduce the ionic conductivity of the electrolyte materials. Xu *et al.*[159] pioneered the use of microwave sintering technology to prepare a P-SOFC electrolyte membrane, which effectively solved the problem of Ba volatilization. This method provides sintering of the BCZY electrolyte densely at 1200 °C, while the traditional sintering method often requires a temperature of 1400 °C. Additionally, microwave-sintered proton conductor (MW-P-SOFC) electrolyte films have more uniform grain distributions and smaller grain sizes than the conventionally sintered proton conductor (C-P-SOFC) electrolyte films. Generally, the larger the grain size, the smaller the volume of protons passing through the grain boundary, and the higher the electrical conductivity. However, in the case of a smaller grain size, the electrical conductivity was found to increase. The main reasons for the conductivity increase are as follows: (1) the microwave sintering method makes the element distribution uniform, restrains the evaporation of Ba^{2+}, thus reducing the activation energy of the grain boundary and improving the electrical conductivity of the grain boundaries. The activation energy of was 0.58 eV (MW-P-SOFC) and 0.68 eV (C-P-SOFC); (2) The lower microwave sintering temperature (1200 °C) effectively prevents the volatilization of electrolyte elements without producing secondary-phase Y_2O_3, as shown in Fig. 11. Yttrium oxide (Y_2O_3) is a non-proton-conducting material. Its presence hinders the conduction process of protons and reduces the electrical conductivity of the material. The specific conduction process is shown in Fig. 12. Due to the high proton electron conductivity, a single cell with

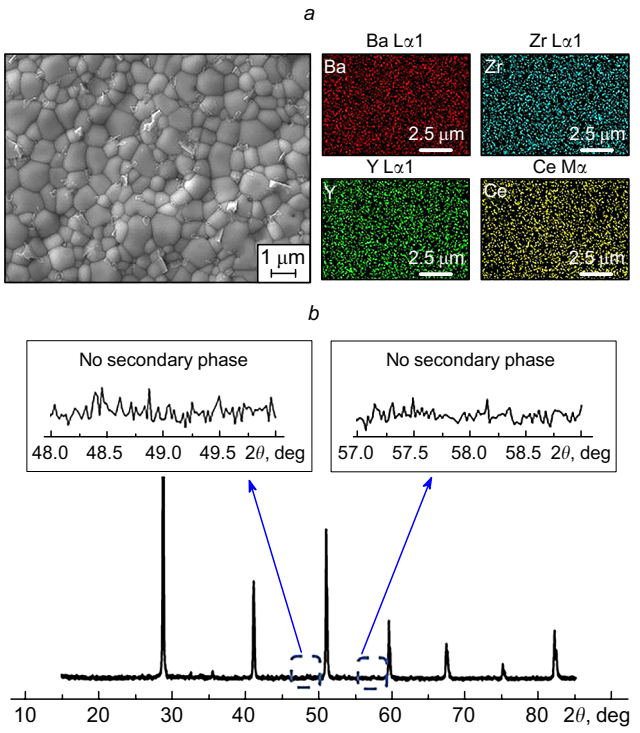


Figure 11. SEM–EDS elemental mapping images (*a*) and XRD pattern for the surface of the BCZY membrane prepared by the microwave sintering method (*b*). Reproduced from Ref. 159 with permission from Elsevier.

MW-P-SOFC as the electrolyte had a higher power density than a single cell with C-P-SOFC. At test temperature of 700 °C, the power density was 838 mW cm^{-2} for MW-P-SOFC and 645 mW cm^{-2} for C-P-SOFC.

However, in the above-mentioned study, only the densification preparation of a P-SOFC electrolyte membrane by microwave sintering has been developed, but the effect of the microwave sintering method on the synthesis of proton conductor oxide powders was not clarified. On the basis of these findings, Wang *et al.*[160] prepared $BaZr_{0.1}Ce_{0.7}Y_{0.2}O_{3-\delta}$ powder by a microwave sintering method and used it for the subsequent preparation of a proton-conducting SOFC electrolyte. The initial particle size of the BZCY powder prepared by microwave sintering was smaller than that of the powder prepared using the CH technology, which was more conducive to the preparation of a high-quality BZCY electrolyte membrane with high compactness and good grain growth, as shown in Figs 13,

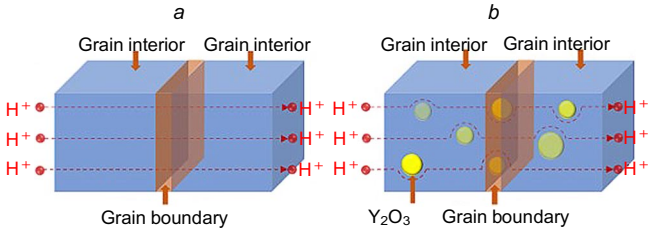


Figure 12. Schematic diagrams of proton transportation in the BCZY membrane prepared by the microwave sintering method (*a*) and the conventional sintering method (*b*). Reproduced from Ref. 159 with permission from Elsevier.

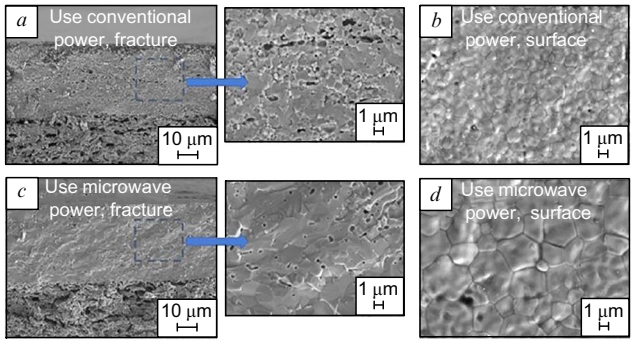


Figure 13. FESEM images of the cross-section (*a*) and surface of the BZCY membrane prepared from the conventionally calcined powder (*b*), and cross-section (*c*) and surface of the BZCY membrane prepared from the microwave-calcined powder (*d*).[160] Reproduced with permission from Elsevier.

14, which illustrate the electrochemical performance of BZCY single cells obtained *via* two said sintering procedures. The results show that the microwave-sintered BCZY powder had a higher power density and open circuit voltage (OCV) than the conventionally sintered powder, which is more suitable for fuel cell applications.

In recent years, $BaCe_{0.7}Zr_{0.1}Y_{0.1}Yb_{0.1}O_{3-\delta}$ (BCZYYb) has been regarded as a good proton-conducting electrolyte material with good performance due to its excellent electrical conductivity and high resistance to CO_2 and

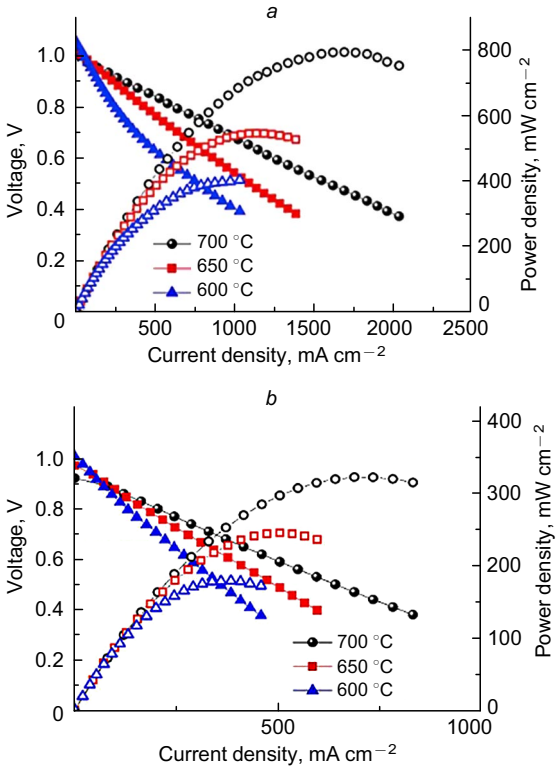


Figure 14. Current–voltage and power density curves for the cell using the BZCY electrolyte membrane made ofthe microwave-calcined powder measured at different temperatures (*a*) and current–voltage and power density curves for the cell using the BZCY electrolyte membrane made of the conventionally sintered powder measured at different temperatures (*b*).[160] Reproduced with permission from Elsevier.

H_2O.[161–163] However, BCZYYb usually requires high sintering densification temperature ($\geqslant$1550 °C) and long sintering time ($\geqslant$10h), which inevitably leads to the volatilization of Ba element, decreases the electrical conductivity of the material,[164, 165] and seriously limits its practical application value. To solve this issue, Zhong *et al.*[166] used MH technology (1400 °C, 2 h, microwave muffle furnace) to prepare a dense BCZYYb electrolyte material with a relative density of 97.6%. At the same time, compared with the traditional sintering method, the sintering densification temperature of this method was reduced by 150 °C. As it can be seen from Table 4, the microwave sintering technology effectively inhibits the volatilization of the Ba element. More importantly, the resulting BCZYYb had high electrical conductivity (3.8×10^{-2} S cm^{-1}, 700 °C). Thus, at 700 °C, using the microwave sintered BCZYYb as the electrolyte, a single cell could reach an excellent maximum power density of 0.64 W cm^{-2}.

Compared with the traditional SOFC preparation process, the process with one sintering step (one-step co-firing method) is a new promising power-saving technology.[167–169] However, the one-step co-firing method faces great challenges. Co-sintering the entire SOFC at high temperatures can densify the electrolyte, but considerable grain growth occurs in the cathode, significantly compromising the catalytic activity of the cathode. Too low co-sintering temperature prevents the electrolyte membrane from being sintered densely, which cannot meet the electrolyte requirements of SOFCs because proton conductor oxides usually require high-temperature sintering ($\geqslant$1400 °C).[170, 171] Due to this challenge, the one-step co-firing technique for fabricating proton conductor SOFCs has not been extensively studied. To reduce the one-step sintering temperature and improve the performance of the prepared cell, Wang *et al.*[172] used $BaZr_{0.1}Ce_{0.66}Ni_{0.04}Y_{0.2}O_{3-\delta}$ as an electrolyte material and $Sm_{0.5}Sr_{0.5}CoO_{3-\delta}$ as a cathode material and employed microwave sintering technology instead of traditional high-temperature furnace sintering to prepare a proton conductor solid oxide fuel cell in a one-step procedure. The effect of microwave sintering technology on the performance of the resulting cell was studied. The results showed that this procedure overcame the difficulty of one-step co-sintering cell preparation technology, and a dense electrolyte film was prepared at a lower sintering temperature (1100 °C) while maintaining the high porosity of the cathode. It is worth emphasizing that the power density of

Table 4. Atomic concentrations representatively measured by EDS and calculated Ba/(Ba + Zr + Ce + Y + Yb) values.[166]

Elements	Stoichiometric BZCYYb	MH (1400 °C)	CH (1550 °C)
Ba (at.%)	50.00	50.77 ± 1.03	36.66 ± 0.39
Zr (at.%)	5.00	5.67 ± 0.42	9.82 ± 1.23
Ce (at.%)	35.00	33.87 ± 0.78	39.46 ± 1.48
Y (at.%)	5.00	5.03 ± 0.39	8.11 ± 0.89
Yb (at.%)	5.00	4.67 ± 0.51	5.92 ± 1.22
Ba/(Ba + Zr + Ce + Y + Yb)	1.00	1.03 ± 0.02	0.58±0.02

Table 5. Selected data on the application of MH technology in SOFC electrolytes.

Composition	Preparation of the precursor	Sintering method	Sintering conditions	Conductivity, S cm^{-1}	Density or relative density	Ref.
$Zr_{0.92}Y_{0.08}O_{0.196}$	Co-precipitation method	MH	1400 °C/20 min	$\sim 1.5 \times 10^{-3}$ (700 °C)	$\sim$5.7 g cm^{-3}	59
10SSZ	Solid-state method	MH	1400 °C/20 min	1.46×10^{-3} (500 °C)	5.46 g cm^{-3}	65
10Sc1CeSZ	MW-NGM	CH	1400 °C/5h	1.84×10^{-2} (800 °C)	NM	73
10Sc1CeSZ	Purchased	MH	1350 °C/15 min	3.14×10^{-2} (800 °C)	$\sim$5.74 g cm^{-3}	74
10GDC	MW-NGM	MH	1200 °C/4 h	3.55×10^{-1} (800 °C)	6.98 g cm^{-3}	98
DDC15	Combustion synthesis by MH	MH	1050 °C/1 h	7.42×10^{-2} (550 °C)	$\sim$95%	99
$Ce_{0.8}Bi_{0.2}O_{2-\delta}$	Self-propagating room temperature procedure	MH	1050 °C/1 h	3.27×10^{-3} (700 °C)	7.63 g cm^{-3}	101
$Ce_{0.8}Sm_{0.1}Y_{0.1}O_{2-\delta}$	Sol–gel auto-combustion synthesis	MH	1200 °C/1 h	2.5×10^{-2} (600 °C)	96.2%	106
$Ce_{0.8}Y_{0.1}Dy_{0.1}O_{2-\delta}$	Sol–gel auto-combustion synthesis	MH	1300 °C/30 min	7.5×10^{-3} (500 °C)	97.1%	108
$Ce_{0.76}Pr_{0.08}Sm_{0.08}Gd_{0.08}O_{2-\delta}$	Sol–gel auto-combustion synthesis	MH	1300 °C/30 min	3.47×10^{-2} (600 °C)	NM	110
$La_{0.8}Sr_{0.2}Ga_{0.83}Mg_{0.17}O_{2.815}$	Microwave-induced solution-polymerization synthesis	MH	1400 °C/9 h	NM	6.45 g cm^{-3}	127
$La_{0.8}Sr_{0.2}(Ga_{0.9}Co_{0.1})_{0.83}$. .$Mg_{0.17}O_{2.815}$	Microwave-induced solution-polymerization synthesis	MH	1400 °C/9 h	NM	6.3 g cm^{-3}	
$La_{0.8}Sr_{0.2}Ga_{0.83}Mg_{0.17}O_{2.815}$	Microwave-induced polysolution polymerization	CH	1400 °C/9 h	NM	6.19 g cm^{-3}	129
$La_2Mo_2O_9$	Microwave-assisted combustion synthesis	CH	800 °C/5 h	0.15S cm^{-1} (750 °C)	97%	140
$La_{1.7}Sm_{0.3}Mo_2O_9$	Microwave-assisted combustion synthesis	CH	800 °C/5 h	0.196S cm^{-1} (750 °C)	98%	141
$BaCe_{0.7}Zr_{0.1}Y_{0.2}O_{3-\delta}$	Combustion method	MH	1200 °C/2 h	1.4×10^{-2} (700 °C)	NM	159
$BaZr_{0.1}Ce_{0.7}Y_{0.1}Yb_{0.1}O_{3-\delta}$	Solid-state method	MH	1400 °C/2 h	3.8×10^{-2} (700 °C)	97.6%	166

Note. NM is not measured.

the cell prepared by microwave one-step co-sintering at 700 °C was 449 mW cm^{-2}, its electrochemical performance was much higher than that of the cell prepared by traditional high-temperature furnace one-step co-sintering (292 mW cm^{-2}), and its output power was higher than that of the previously reported one-step co-sintered cell.[169, 173, 174] At the same time, the co-firing temperature of 1100 °C used in this study was the lowest reported temperature for the densification of BZCY-based electrolytes. Therefore,microwave sintering provides an effective approach to the proton conductor SOFCs by a one-step co-sintering technology.

Table 5 summarizes some important data on the application of MH technology in SOFC electrolytes, which is convenient for readers to analyze more clearly and quickly.

4. Conclusion

Due of its fast and uniform heating mode, MH technology can not only save energy but also effectively solve the problems of uneven grain growth and element volatilization during synthesis and sintering of the solid state electrolyte (or other conducting ceramics). In addition, compared with CH technology, MH technology enables lower phase formation and sintering densification temperatures of electrolyte materials, improves the microstructures of the electrolytes, promotes the densification of grains, reduces the activation energy between electrolyte grain boundaries, and improves the conductivities of the electrolytes.

MH technology was initially applied to SOFC electrolytes to form a system, but the rapid microwave sintering of electrolytes was only attributed to the unique effect of the microwave field, which does not provide a perfect explanation at the micro level. Many studies have only put forward assumptions but have not clarified the mechanism of action of each factor. Energy savings have been identified as the main advantage of using MH for electrolyte sintering, and its contribution to the electrolyte conductivity enhancement is still not very clear. Some studies have indicated that the conventionally recognized attainment of small grains by MH may not always be correct, as the small grains are the result of the lower sintering temperature and shorter dwelling time. The low sintering temperature could restrict the elemental evaporation, which would be beneficial for the enhancement of the electrolyte conductivity. Using the MH method at the same sintering temperature and dwelling time as those used in the CH method makes it highly possible to obtain a larger grain size of the electrolyte, although the severity of the elemental evaporation under such conditions is not clear. Therefore, it would be necessary to achieve a balance between grain growth and elemental evaporation by suitably tuning the microwave sintering temperature. In addition, increasing or decreasing the grain size to influence the electrolyte conductivity is the traditional but also preliminary way of tailoring the electrolyte conductivity. Since the microwave sintering involves a heating method other than conventional sintering, the defects formed at the grain interiors or grain boundaries may influence the electrolyte conductivity. Furthermore, beyond the total volume of the grain boundaries, the microwave sintering can also affect the thickness of each grain boundary, which is usually in the range of a few nanometres. Therefore, many areas, including defect chemistry and electrolyte microstructures from the nanometre to the micrometre scale, can be studied in the future. At the same time, the determination of the electromagnetic field involved in the electrolyte sintering process and the dielectric parameters of the material also needs to be improved to better utilize microwave sintering.

Microwave heating is induced by the loss of electric field energy of the dielectric material. The thermal effects of various dielectric materials under the action of microwave electromagnetic fields are different. Based on this fact, the determination of whether MH technology can be used in the densification sintering of double-layer SOFCs and which double-layer electrolyte materials are suitable for MH technology is an important area ofresearch. In addition, MH technology is more widely used in the sintering and preparation of O-SOFC electrolytes. Nevertheless, few studies have been reported on proton-conducting electrolytes, especially the effect of MH technology on the performance of P-SOFC electrolyte precursors, and the mechanisms of action on grains and grain boundaries need to be further discussed. Considering that proton-conducting oxides are becoming the hottest topic in the SOFC field, it could be interesting to actively explore the utilization of MH for proton-conducting oxides, which not only offers a new route for the preparation of proton-conducting oxides but also may give rise to new features of the proton-conducting oxides induced by microwave sintering.

Although MH technology has the advantages of faster heating rate and reduced environmental hazards and improves the mechanical properties of materials compared with CH technology, the most significant drawback of MH is that it cannot be used to heat metals.[175] Table 6 summarizes the advantages and disadvantages of CH and MH in more detail.

Table 6. The advantages and disadvantages of CH and MH techniques.

Method	Advantage	Disadvantage
MH	Fast heating rates Minimum energy consumption Decreased processing time Reduced environmental hazards	Cannot heat metals
CH	A wide range of trials Low cost of equipment Good heat preservation performance	Non-uniform heating Slow heating rate High energy consumption

5. List of acronyms and designations

BCZY — $BaZr_{0.1}Ce_{0.7}Y_{0.2}O_{3-\delta}$,
CeSZ — ceria-stabilized zirconi,
CH — conventional heating,
C-P-SOFC — conventionally sintered proton conductor,
DDC — dysprosium-doped cerium oxides,
EDS — energy dispersive X-ray spectroscopy,
FESEM — field emission scanning emission microscopy,
GDC — gadolinium-doped ceria,
IT-SOFC — intermediate-temperature SOFC,
LSGM — $La_{0.9}Sr_{0.1}Ga_{0.8}Mg_{0.2}O_{3-\delta}$,
MH — microwave heating,
MW — microwave sintering,
MW-NGM — microwave-assisted nitrate glycine method,

MWP — microwave-assisted Pechini method,
MW-P-SOFC — microwave-sintered proton conductor,
MW-SGP — microwave-assisted sol–gel Pechini method,
NDC — neodymium-doped ceria,
O-SOFC — ion-conducting SOFC electrolytes,
P-SOFC — proton-conducting SOFC electrolytes,
PSZ — partially stabilized ZrO_2,
PVA — polyvinyl alcohol,
ScSZ — scandia-stabilized zirconia,
SDC — samarium-doped ceria,
SEM — scanning electron microscopy,
SOFC — solid oxide fuel cells,
3Y-nLa-PSZ — 3 mol.% Y_2O_3 and n mol.% La_2O_3 (n = 0, 1, 3, 5) co-doped partially stabilized ZrO_2,
YSZ — yttria-stabilized zirconia

6. References

1. Y.Zhang, J.Mei, C.Yan, T.Liao, J.Bell, Z.Sun. *Adv. Mater.*, **32**, 1902806 (2020)
2. Y.Li, Y.Sun, Y.Qin, W.Zhang, L.Wang, M.Luo, H.Yang, S.Guo. *Adv. Energy Mater.*, **10**, 1903120 (2020)
3. C.Peng, P.Wei, X.Li, Y.Liu, Y.Cao, H.Wang, H.Yu, F.Peng, L.Zhang, B.Zhang. *Nano Energy*, **53**, 97 (2018)
4. J.Ma, Y.Kong, S.Liu, Y.Li, J.Jiang, Q. Zhou, Y.Huang, S.Han. *ACS Appl. Energy Mater.*, **3**, 11900 (2020)
5. J.Ling, Y.Zhou, W.Xu, H.Lin, S.Lu, B.Wang, K.Wang. *J. Adv. Ceram.*, **9**, 45 (2020)
6. S.Yu, Y.Wang, L.Bi. *Ceram. Int.*, **48**, 17987 (2022)
7. A.Sajid, E.Pervaiz, H.Ali, T.Noor, M.M.Baig. *Int. J. Energy Res.*, **46**, 6953 (2022)
8. Y.Xu, X.Liu, N.Cao, X.Xu, L.Bi. *Sustain Mater. Technol.*, **27**, e00229 (2021)
9. Y.Xu, X.Xu, N.Cao, X.Wang, X.Liu, M.Fronzi, L.Bi. *Int. J. Hydrogen Energy*, **46**, 10293 (2021)
10. D.Xie, K.Li, J.Yang, D.Yan, L.Jia, B.Chi, J.Pu, J.Li. *Int. J. Hydrogen Energy*, **46**, 10007 (2021)
11. I.Zvonareva, X.-Z.Fu, D.Medvedev, Z.Shao. *Energy Environ. Sci.*, **15**, 439 (2022)
12. A.Dehghani-Sanij, E.Tharumalingam, M.Dusseault, R.Fraser. *Renewable Sustainable Energy Rev.*, **104**, 192 (2019)
13. L.Fan, B.Zhu, P.-C.Su, C.He. *Nano Energy*, **45**, 148 (2018)
14. T.Wei, P.Qiu, J.Yang, L.Jia, B.Chi, J.Pu, J.Li. *J.Power Sources*, **484**, 229199 (2021)
15. M.Shahid. *Ionics*, **28**, 3583 (2022)
16. S.Li, J.T.Irvine. *Solid State Ionics*, **361**, 115571 (2021)
17. A.S.Kumar, R.Balaji, S.Jayakumar. *Fuel*, **21**, 23 (2018)
18. S.P.Badwal, F.T.Ciacchi, K.M.Giampietro. *Solid State Ionics*, **176**, 169 (2005)
19. S.Badwal, S.Jiang, J.Love, J.Nowotny, M.Rekas, E.Vance. *Ceram. Int.*, **27**, 419 (2001)
20. S.Badwal. *Solid State Ionics*, **76**, 67 (1995)
21. S.Badwal. *J. Mater. Sci.*, **19**, 1767 (1984)
22. S.Badwal. *Appl. Phys. A*, **50**, 449 (1990)
23. N.Danilov, E.Pikalova, J.Lyagaeva, B.Antonov, D.Medvedev, A.Demin, P.Tsiakaras. *J. Power Sources*, **366**, 161 (2017)
24. Y.Chen, Y.Fan, S.Lee, G.Hackett, H.Abernathy, K.Gerdes, X.Song. *J. Power Sources*, **438**, 227043 (2019)
25. X.Guo, R.Waser. *Prog. Mater. Sci.*, **51**, 151 (2006)
26. C.Kjølseth, H.Fjeld, Ø.Prytz, P.I.Dahl, C.Estournès, R.Haugsrud, T.Norby. *Solid State Ionics*, **181**, 268 (2010)
27. M.Chen, X.Xie, J.Guo, D.Chen, Q. Xu. *J. Mater. Chem. A*, **8**, 12566 (2020)
28. S.Hussain, L.Yangping. *Energy Transitions*, **4**, 113 (2020)
29. S.Y.Toor, E.Croiset. *Ceram. Int.*, **46**, 1148 (2020)
30. S.Dwivedi. *Int. J. Hydrogen Energy*, **45**, 23988 (2020)
31. A.S.Vanetsev, A.V.Orlov, Y.D.Tretyakov. *MRS Online Proceedings Library (OPL)*, **906** (2005)
32. G. Yang, S.-J.Park. *Materials*, **12**, 3631 (2019)
33. L.Ćurković, R.Veseli, I. Gabelica, I. Žmak, I. Ropuš, M.Vukšić. *Trans. Famena*, **45**, 1 (2021)
34. M.Gupta, S.Shirbhate, P.Ojha, S.Acharya. *Solid State Ionics*, **320**, 199 (2018)
35. M.R.Cesário, E.Savary, S.Marinel, B.Raveau, V. Caignaert. *Solid State Ionics*, **294**, 67 (2016)
36. A.S.Kumar, R.Balaji, S.Jayakumar, C.Pradeep. *Mater. Chem. Phys.*, **182**, 520 (2016)
37. S.S.B.C.Abdullah, T.Teranishi, H.Hayashi, A.Kishimoto. *J. Power Sources*, **374**, 92 (2018)
38. M.Yoshinaga, T.Sasaki, N.Kobayashi. *J. Ceram. Soc. Jpn.*, **127**, 767 (2019)
39. A.Borrell, M.D.Salvador. *Sinter. Technol. Method Appl.*, 3 (2018)
40. V.G. Karayannis. *IOP Conf. Ser.: Mater. Sci. Eng.*, **161**, 12068 (2016)
41. R.R.Menezes, P.M.Souto, R.Kiminami. *Sintering of Ceramics — New Emerging Techniques*. A.Lakshmanan, Croatia, 3 (2012)
42. D.Agrawal. *Sintering of Advanced Materials*. Elsevier, 222 (2010)
43. D.Xie, A.Ling, D.Yan, L.Jia, B.Chi, J.Pu, J.Li. *Electrochim. Acta*, **344**, 136143 (2020)
44. P.P.Fedorov, E.G.Yarotskaya. *Condens. Matter Interphases*, **23**, 170 (2021)
45. T.Politova, J.T.Irvine. *Solid State Ionics*, **168**, 153 (2004)
46. Z.Zakaria, S.K.Kamarudin. *Int. J. Energy Res.*, **45**, 4871 (2021)
47. S.-h.Guan, Z.-p.Liu. *Chin. J. Chem. Phys.*, **34**, 125 (2021)
48. A.O.Zhigachev, V.V.Rodaev, D.V.Zhigacheva, N.V.Lyskov, M.A.Shchukina. *Ceram. Int.*, **47**, 32490 (2021)
49. D.Panthi, N.Hedayat, Y.Du. *J. Adv. Ceram.*, **7**, 325 (2018)
50. M.J.Son, M.W.Kim, A.V.Virkar, H.-T.Lim. *Electrochim. Acta*, **353**, 136450 (2020)
51. M.Yoshimura, T.Hiuga, S.Sōmiya. *J. Cryst. Growth*, **71**, 277 (1985)
52. A.R.Arakaki, W.K.Yoshito, V.Ussui, D.R.R.Lazar. *Mater. Sci. Forum*, **660**, 983 (2010).
53. O.Bohnke, V.Gunes, K.V.Kravchyk, A.G.Belous, O.Z.Yanchevskii, O.I. V'Yunov. *Solid State Ionics*, **262**, 517 (2014)
54. J.Xiao, Q.Han, F.Yu, Y.Zhang, H.Wu, X.Li, X.Zeng, P.Dong, Y.Zhang, J.Liu. *J. Alloys Compd.*, **731**, 1080 (2018)
55. H.M.Mirabad, A.Nemati, M.A.Faghihi-Sani, M.F.Hasanabadi, H.Abdoli. *J. Alloys Compd.*, **847**, 156496 (2020)
56. A.Beketova, A.Theocharidou, I. Tsamesidis, A.E.Rigos, G.K.Pouroutzidou, E.-G.C.Tzanakakis, D.Kourtidou, L.Liverani, M.A.Ospina, A.Anastasiou, I.G.Tzoutzas, E.Kontonasaki. *Dent. J.*, **9**, 128 (2021)
57. N.Q.Minh. *J. Am. Ceram. Soc.*, **76**, 563 (1993)
58. S.K.Vijay, V.Chandramouli, S.Khan, P.C.Clinsha, S.Anthonysamy. *Ceram. Int.*, **40**, 16689 (2014)
59. K.L.Singh, P.Sharma, A.P.Singh, A.Kumar, S.S.Sekhon. *JOM*, **69**, 2448 (2017)
60. Y.Chen, B.Fan, B.Yang, W.Ma, G.Liu, H.Li. *Ceram. Int.*, **45**, 17675 (2019)
61. J.Jiang, J.L.Hertz. *J. Electroceram.*, **32**, 37 (2014)
62. G.Y.Cho, Y.H.Lee, S.W.Hong, J.Bae, J.An, Y.B.Kim, S.W.Cha. *Int. J. Hydrogen Energy*, **40**, 15704 (2015)
63. J.H.Joo, G.M.Choi. *Solid State Ionics*, **180**, 252(2009)
64. H.Ao, X.Liu, H.Zhang, J.Zhou, X.Huang, Z.Feng, H.Xu. *J. Rare Earths*, **33**, 746 (2015)
65. P.Sharma, K.L.Singh, A.P.Singh, C.Sharma, S.Mago. *Trans. Indian Ceram. Soc.*, **78**, 20 (2019)
66. S.Kazlauskas, A.Kezionis, E.Kazakevicius, A.F.Orliukas. *Electrochim. Acta*, **134**, 176 (2014)
67. D.J.Brett, A.Atkinson, N.P.Brandon, S.J.Skinner. *Chem. Soc. Rev.*, **37**, 1568 (2008)

68. D.Lee, I.Lee, Y.Jeon, R.Song. *Solid State Ionics*, **176**, 1021 (2005)
69. Q.Xue, X.Huang, L.Wang, H.Zhang, J.Zhang. *Phys. Rev. Appl.*, **10**, 014032 (2018)
70. H.P.Dasari, J.S.Ahn, K.Ahn, S.-Y.Park, J.Hong, H.Kim, K.J.Yoon, J.-W.Son, H.-W.Lee, J.-H.Lee. *Solid State Ionics*, **263**, 103 (2014)
71. J.Tan, Y.Su, H.Tang, T.Hu, Q.Yu, R.Tursun, X.Zhang. *J. Alloys Compd.*, **686**, 394 (2016)
72. R.A.Richardson, J.W.Cotton, R.Mark Ormerod. *Dalton Trans.*, **19**, 3110 (2004)
73. A.A.Jais, S.M.Ali, M.Anwar, M.R.Somalu, A.Muchtar, W.N.R.W.Isahak, C.Y.Tan, R.Singh, N.P.Brandon. *Ceram. Int.*, **43**, 8119 (2017)
74. C.K.Ng, S.Ramesh, C.Y.Tan, A.Muchtar, M.R.Somalu. *Int. J. Hydrogen Energy*, **41**, 14184 (2016)
75. E.Y.Pikalova, E.G.Kalinina. *Russ. Chem. Rev.*, **90**, 703 (2021)
76. T.K.Maiti, J.Majhi, S.K.Maiti, J.Singh, P.Dixit, T.Rohilla, S.Ghosh, S.Bhushan, S.Chattopadhyay. *Environ. Sci. Pollut. Res.*, **208**, 1 (2022)
77. J.D.C.Carregosa, J.P.F.Grilo, G.S.Godoi, D.A.Macedo, R.M.Nascimento, R.M.P.B.Oliveira. *Ceram. Int.*, **46**, 23271 (2020)
78. Z.Liu, B.Wang, C.Cazorla. *Materialia*, **15**, 101050 (2021)
79. J.Kang, W.Feng, D.Guo, K.Chen, S.Gao, J.Jiang, C.Lu, B.Niu, B.Wang. *J. Alloys Compd.*, **913**, 165317 (2022)
80. M.Dudek, M.Mróz, Ł.Zych, E.Drozdz-Cieśla. *Mater. Sci.-Pol.*, **26**, 319 (2008)
81. J.Cheng, Q.Jiang, H.He, J.Yang, Y.Wang, J.Gao. *Mater. Chem. Phys.*, **125**, 704 (2011)
82. D.Medvedev, V.Maragou, E.Pikalova, A.Demin, P.Tsiakaras. *J. Power Sources*, **221**, 217 (2013)
83. M.Farahmandjou, M.Dastpak. *Phys. Chem. Res.*, **6**, 713 (2018)
84. L.Li, B.Zhu, J.Zhang, C.Yan, Y.Wu. *Int. J.Hydrogen Energy*, **43**, 12909 (2018)
85. I.Díaz-Aburto, F.Gracia, M.Colet-Lagrille. *Fuel Cells*, **19**, 147 (2019)
86. D.Y.Chung, E.H.Lee. *J. Alloys Compd.*, **374**, 69 (2004)
87. J.Prado-Gonjal, R.Schmidt, J.Espíndola-Canuto, P.Ramos-Alvarez, E.Morán. *J. Power Sources*, **209**, 163 (2012)
88. I.Shajahan, H.P.Dasari, P.Govardhan. *Mater. Chem. Phys.*, **240**, 122211 (2020)
89. M.K.Ullah, N.Ahmad, S.U.-D.Khan, F.Alvi, G.Abbas, A.Rafique, A.Ali, M.A.Ahmad, R.Raza. *Int. J. Hydrogen Energy*, **44**, 10964 (2019)
90. F.Bondioli, A.M.Ferrari, C.Leonelli, C.Siligardi, N.A.Hart, N.G.Evans. *J. Mater. Chem.*, **11**, 2620 (2001)
91. Y.-f.Bu, Q.Zhong, W.-y.Tan, R.-j.Zhou, Y.Song, W.Cai. *Mater. Sci. Semicond. Process.*, **16**, 2058 (2013)
92. A.Arabaci, Ö.Serin. *J. Mater. Eng. Perform.*, **24**, 2730 (2015)
93. N.Jaiswal, K.Tanwar, R.Suman, D.Kumar, S.Upadhyay, O.Parkash. *J. Alloys Compd.*, **781**, 984 (2019)
94. D.Puente-Martínez, J.Díaz-Guillén, S.Montemayor, J.Díaz-Guillén, O.Burciaga-Díaz, M.Bazaldúa-Medellín, M.Diaz-Guillen, A.Fuentes. *Int. J. Hydrogen Energy*, **45**, 14062 (2020)
95. J.Zheng, H.Zhu, W.Li, Z.Ma, X.Ou, Y.Fan, Y.Guo, X.Wang, Y.Ling. *Int. J. Hydrogen Energy*, **46**, 13318 (2021)
96. V.Sal'nikov, E.Y.Pikalova. *Phys. Solid State*, **57**, 1944 (2015)
97. M.A.Rana, M.Akbar, M.Anwar, K.Mustafa. *Mater. Today: Proc.*, **2**, 5649 (2015)
98. S.P.S.Shaikh, C.V.Rode. *RSC Adv.*, **10**, 3020 (2020)
99. S.A.Acharya. *J. Power Sources*, **198**, 105 (2012)
100. Z.-C.Li, H.Zhang, B.Bergman. *Ceram. Int.*, **34**, 1949 (2008)
101. M.Prekajski, M.Stojmenović, A.Radojković, G.Branković, H.Oraon, R.Subasri, B.Matović. *J. Alloys Compd.*, **617**, 563 (2014)
102. F.-Y.Wang, S.Chen, S.Cheng. *Electrochem. Commun.*, **6**, 743 (2004)
103. X.Wei, G.Hou, Y.An, P.Yang, X.Zhao, H.Zhou, J.Chen. *Ceram. Int.*, **47**, 6875(2021)
104. X.Sha, Z.Lü, X.Huang, J.Miao, Z.Liu, X.Xin, Y.Zhang, W.Su. *J. Alloys Compd.*, **433**, 274 (2007)
105. Y.Xue, S.An, S.Li, J.Peng, C.Cai, Y.Liu. *J. Solid State Electrochem.*, **24**, 1639 (2020)
106. K.Venkataramana, K.Ravindranath, C.Madhuri, C.Madhusudan, N.Pavan Kumar, C.Vishnuvardhan Reddy. *Ionics*, **24**, 1429 (2018)
107. S.Tadokoro, E.Muccillo. *J. Eur. Ceram. Soc.*, **27**, 4261 (2007)
108. C.Madhusudan, V.Kasarapu, M.Chittimadula, Y.S.Reddy, C.V.Reddy. *Rare Met.*, **40**, 3329 (2021)
109. K.Venkataramana, C.Madhuri, Y.S.Reddy, G.Bhikshamaiah, C.V.Reddy. *J. Alloys Compd.*, **719**, 97 (2017)
110. K.Venkataramana, C.Madhuri, J.Shanker, C.Madhusudan, C.Vishnuvardhan Reddy. *Ionics*, **24**, 3075 (2018)
111. J.Prado-Gonjal, R.Heuguet, D.Munoz-Gil, A.Rivera-Calzada, S.Marinel, E.Moran, R.Schmidt. *Int. J. Hydrogen Energy*, **40**, 15640 (2015)
112. E.Filonova, D.Medvedev. *Nanomaterials*, **12**, 1991 (2022)
113. S.Yu, H.Bi, J.Sun, L.Zhu, H.Yu, C.Lu, X.Liu. *J. Alloys Compd.*, **777**, 244 (2019)
114. K.Hosoi, T.Sakai, S.Ida, T.Ishihara. *Electrochim. Acta*, **194**, 473 (2016)
115. T.Ishihara, H.Matsuda, Y.Takita. *J. Am. Chem. Soc.*, **116**, 3801 (1994)
116. P.-n. Huang, A.Petric. *J. Electrochem. Soc.*, **143**, 1644 (1996)
117. T.Ishihara, J.Tabuchi, S.Ishikawa, J.Yan, M.Enoki, H.Matsumoto. *Solid State Ionics*, **177**, 1949 (2006)
118. Z.Naiqing, S.Kening, Z.Derui, J.Dechang. *J. Rare Earths*, **24**, 90 (2006)
119. K.Huang, M.Feng, J.B.Goodenough. *J. Am. Ceram. Soc.*, **79**, 1100 (1996)
120. I.Stijepovic, A.Darbandi, V.Srdic. *J. Optoelectron. Adv. Mater.*, **12**, 1098 (2010)
121. M.Shi, Y.Xu, A.Liu, N.Liu, C.Wang, P.Majewski, F.Aldinger. *Mater. Chem. Phys.*, **114**, 43 (2009)
122. L.Cong, T.He, Y.Ji, P.Guan, Y.Huang, W.Su. *J. Alloys Compd.*, **348**, 325 (2003)
123. M.Shi, N.Liu, Y.Xu, Y.Yuan, P.Majewski, F.Aldinger. *J. Alloys Compd.*, **425**, 348 (2006)
124. A.Tarancón, G.Dezanneau, J.Arbiol, F.Peiró, J.Morante. *J. Power Sources*, **118**, 256 (2003)
125. N.Liu, Y.Yuan, P.Majewski, F.Aldinger. *Mater. Res. Bull.*, **41**, 461 (2006)
126. V.A.Kolotygin, I.E.Kuritsyna, N.V.Lyskov. *Catal. Mater. Hydrog. Prod. Electro-Oxidation React.*, **2**, 198 (2018)
127. Y.Zhai, C.Ye, J.Xiao, L.Dai. *J. Power Sources*, **163**, 316 (2006)
128. S.Boldrini, C.Mortalo, S.Fasolin, F.Agresti, L.Doubova, M.Fabrizio, S.Barison. *Fuel Cells*, **12**, 54 (2012)
129. Y.Zhai, C.Ye, F.Xia, J.Xiao, L.Dai, Y.Yang, Y.Wang. *J. Power Sources*, **162**, 146 (2006)
130. R.Subasri, T.Mathews, O.Sreedharan. *Mater. Lett.*, **57**, 1792 (2003)
131. S.Kesapragada, S.Bhaduri, S.Bhaduri, P.Singh. *J. Power Sources*, **124**, 499 (2003)
132. A.Moure, A.Castro, J.Tartaj, C.Moure. *J. Power Sources*, **188**, 489 (2009)
133. S.Nakayama, M.Sakamoto. *J. Eur. Ceram. Soc.*, **18**, 1413 (1998)
134. Y.Higuchi, M.Sugawara, K.Onishi, M.Sakamoto, S.Nakayama. *Ceram. Int.*, **36**, 955 (2010)
135. L.Leon-Reina, M.Martin-Sedeno, E.Losilla, A.Cabeza, M.Martinez-Lara, S.Bruque, F.Marques, D.Sheptyakov, M.Aranda. *Chem. Mater.*, **15**, 2099 (2003)
136. M.Santos, C.Alves, F.A.C.Oliveira, T.Marcelo, J.Mascarenhas, A.Cavaleiro, B.Trindade. *J. Power Sources*, **231**, 146 (2013)

137. P.Lacorre, F.Goutenoire, O.Bohnke, R.Retoux, Y.Laligant. *Nature (London)*, **404**, 856 (2000)
138. S.Georges, F.Goutenoire, F.Altorfer, D.Sheptyakov, P.Lacorre. *Solid State Ionics*, **161**, 231 (2003)
139. J.Yang, Z.Gu, Z.Wen, D.Yan. *Solid State Ionics*, **176**, 523 (2005)
140. T.Saradha, S.Muzhumathi, A.Subramania. *J. Solid State Electrochem.*, **12**, 143 (2008)
141. T.Saradha, A.Subramania, K.Balakrishnan, S.Muzhumathi. *Mater. Res. Bull.*, **68**, 320 (2015)
142. X.Kuai, G.Yang, Y.Chen, H.Sun, J.Dai, Y.Song, R.Ran, W.Wang, W.Zhou, Z.Shao. *Adv. Energy Mater.*, **9**, 1902384 (2019)
143. M.Xu, J.Yu, Y.Song, R.Ran, W.Wang, Z.Shao. *Energy Fuels*, **34**, 10568 (2020)
144. M.Irshad, R.Idrees, K.Siraj, I. Shakir, M.Rafique, Q.ul Ain, R.Raza. *Int. J.Hydrogen Energy*, **46**, 10448 (2021)
145. M.Irshad, Q.ul Ain, K.Siraj, R.Raza, A.N.Tabish, M.Rafique, R.Idrees, F.Khan, S.Majeed, M.Ahsan. *J. Alloys Compd.*, **815**, 152389 (2020)
146. F.Jin, X.Liu, X.Chu, Y.Shen, J.Li. *J. Mater. Sci.*, **56**, 1147 (2021)
147. F.J.Loureiro, D.A.Macedo, R.M.Nascimento, M.R.Cesario, J.P.Grilo, A.A.Yaremchenko, D.P.Fagg. *J. Eur. Ceram. Soc.*, **39**, 1846 (2019)
148. Y.Yin, S.Yu, H.Dai, L.Bi. *J.Mater. Chem. A*, **10**, 1726 (2022)
149. Y.Xu, X.Xu, L.Bi. *J. Adv. Ceram.*, **11**, 794 (2022)
150. H.Dai, Y.Yin, X.Li, C.Ma, Z.Chen, M.Hua, L.Bi. *Sustain Mater. Technol.*, **32**, e00409 (2022)
151. A.P.Tarutin, J.G.Lyagaeva, D.A.Medvedev, L.Bi, A.A.Yaremchenko. *J. Mater. Chem. A*, **9**, 154 (2021)
152. L.Zhang, Y.Yin, Y.Xu, S.Yu, L.Bi. *Sci. China Mater.*, **65**, 1485 (2022)
153. S.Wu, X.Xu, X.Li, L.Bi. *Sci. China Mater.*, **65**, 675 (2022)
154. M.Fu, K.Li, Q.Zeng, L.Zeng, Z.Tao. *Sep. Purif. Technol.*, **287**, 120581 (2022)
155. J.Hou, G.Yang, W.Liu. *Mater. Res. Bull.*, **150**, 111769 (2022)
156. Z.Tao, X.Xu, L.Bi. *Electrochem. Commun.*, **129**, 107072 (2021)
157. S.Barison, M.Fabrizio, S.Fasolin, F.Montagner, C.Mortalò. *Mater. Res. Bull.*, **45**, 1171 (2010)
158. D.Han, S.Uemura, C.Hiraiwa, M.Majima, T.Uda. *ChemSusChem*, **11**, 4102 (2018)
159. X.Xu, L.Bi, X.Zhao. *J. Membr. Sci.*, **558**, 17 (2018)
160. B.Wang, X.Liu, L.Bi, X.Zhao. *J. Power Sources*, **412**, 664 (2019)
161. S.Wang, Z.Fei, L.Zhang, F.Chen. *Solid State Ionics*, **213**, 29 (2012)
162. L.Yang, K.Blinn, Z.Cheng, M.Liu, M.Liu, Z.Liu, S.Wang. *Science*, **326**, 126 (2009)
163. Z.Fei, J.Chao, C.Yang, S.Wang, F.Chen. *J. Power Sources*, **196**, 688 (2011)
164. H.I.Ji, B.K.Kim, J.W.Son, K.J.Yoon, J.H.Lee. *J. Power Sources*, **507**, 230296 (2021)
165. W.Yang, H.Zhou, L.Wang, Y.Li, L.Dai. *Int. J. Hydrogen Energy*, **46**, 10838 (2021)
166. Z.Zhong, X.Xu, Z.Zhang, J.Li, X.Guo, S.Wu, H.Sun. *Int. J. Hydrogen Energy*, **47**, 25367 (2022)
167. M.Liu, D.Dong, F.Zhao, J.Gao, D.Ding, X.Liu, G.Meng. *J. Power Sources*, **182**, 585 (2008)
168. H.Dai, H.Chen, S.He, G.Cai, L.Guo. *J. Power Sources*, **286**, 427 (2015)
169. H.Dai, H.Kou, Z.Tao, K.Liu, M.Xue, Q.Zhang, L.Bi. *Ceram. Int.*, **46**, 6987 (2020)
170. L.Bi, E.Fabbri, E.Traversa. *Electrochim. Acta*, **260**, 748 (2018)
171. J.Ma, Z.Tao, H.Kou, M.Fronzi, L.Bi. *Ceram. Int.*, **46**, 4000 (2020)
172. B.Wang, L.Bi, X.Zhao. *J. Eur. Ceram. Soc.*, **38**, 5620 (2018)
173. L.Bi, Z.Tao, W.Sun, S.Zhang, R.Peng, W.Liu. *J. Power Sources*, **191**, 428 (2009)
174. W.Sun, Z.Tao, Z.Shi, L.Yan, Z.Zhu, W.Liu. *Fuel Cells*, **10**, 1108 (2010)
175. W.Wang, Z.Liu, J.Sun, Q.Ma, C.Ma, Y.Zhang. *AlChE J.*, **58**, 3852 (2012)